ECS Transactions, 28 (2) 119-126 (2010)
10.1149/1.3372569 ©The Electrochemical Society

Modulation of the Electrical Characteristics of HfOx/TiN RRAM Devices through the Top Electrode Metal

K. M. Chang[a], W. H. Tzeng[a], K. C. Liu[b], W. R. Lai[a]

[a] Department of Electronics Engineering & Institute of Electronics, National Chiao Tung University, HsinChu, 30010, Taiwan
[b] Institute of Electro-Optical Engineering, Chang Gung University, Tao-Yuan, 33302, Taiwan

The effect of the top electrode on switching characteristics of a HfOx/TiN structure was investigated. From the electrical conduction analysis, the conduction mechanism between Pt and Ti was found to be quite different. A potential barrier formed in the Pt/HfOx interface showing the Fowler-Nordheim tunneling at high bias. However, it was not observed in the Ti/HfOx structure. Reactive metal Ti interacted with the underlying HfOx film leading to destruction of the barrier height. As such, the device lost the ability to operate at the μA compliance current range. Pt/HfOx demonstrated the merit of a large resistance ratio and a low operation current (Ireset = 20 μA). However, Ti/HfOx exhibited better voltage dispersion at the low resistance state (0.5V dispersion). The electrode plays a dominant role in determining the electrical characteristics of a resistive random access memory (RRAM) device. Therefore, choosing an adequate electrode for RRAM is an important consideration.

Introduction

Resistive random access memory has attracted much attention in recent years because of its simple structure, low power operation, fast switching speed, and compatibility with the standard complementary metal-oxide semiconductor (CMOS) technology. Many candidate binary oxide materials, such as NiO (1), TiO_2 (2), and ZrO_2 (3) have been proposed, but the mechanism of the switching behavior is not really clear. The electrode effect shows that different switching behaviors need to be investigated to further understand the switching mechanism. Seo et al. (4) proposed that the resistance switching behaviors of NiO/Pt device was dominated by the work function (WF) of the top metal. When the metal/NiO interface, such as Pt/NiO/Pt and Au/NiO/Pt, formed ohmic contact, voltage drops at the interface were omitted, and the effective electric field inside the NiO film was high enough to induce resistance switching. For a Ti/NiO/Pt structure, a well-defined Schottky contact at the Ti/NiO interface leading to an effective electric field inside the NiO film was not enough to induce resistance switching. Lin et al. (5) discussed the effect of the top electrode material on the resistive switching properties of ZrO_2 film. Metal Al and Pt, used as top electrodes, showed unipolar switching with a large dispersion of R_{on}, R_{off}, V_{on}, and V_{off}, while metal Ti showed a stable bipolar switching behavior. Lee et al. (6) proposed that the effect of metal electrodes on NiO RRAM device is correlated to the free energy of the oxide formation between electrode and Ni. It seemed that the top electrode plays an important role in the performance of a RRAM device, depending on the kind of transition metal oxide (TMO) used. HfOx film

with Pt, Au, and Ru metal as the top electrode has been reported to have resistive switching properties (7-9), but not much mention has been made on the effect of the top electrode on a HfOx RRAM device.

In this report, we observed the electrical characteristics of a HfOx/TiN capacitor structure with metal Pt and Ti top electrodes. Distinct electrical behaviors for each metal top electrode were observed. To further understand the effect of the top electrode on the HfOx/TiN device, electrical fitting curves were also investigated. Resistance ratio and operation voltage fluctuation were also discussed. Pt/HfOx/TiN demonstrated the merits of a low leakage current and a low power operation, but Ti did not. From the electrical fitting curves, different conduction behaviors were observed in high resistance state (HRS). The top metal electrode not only altered the type of switching property, but also influenced the operation dispersion and resistance ratio. The effect of the top electrode is crucial to the performance of a HfOx RRAM device.

Experiments

Non-stoichiometric HfOx thin films with a thickness of 30nm were deposited on $TiN/SiO_2/Si$ substrates by atomic layer deposition (ALD) at a temperature of 300℃. Hafnium tetrachloride ($HfCl_4$) and water (H_2O) were used as reactants during ALD. Dc sputtering process was used to deposit the metal electrode with a shadow mask, and the thicknesses of Pt and Ti were set at 1000 Å and 400 Å, respectively. To investigate the reason for the difference in the switching property, the chemical bonding energies were examined by X-ray photoelectron spectroscopy (XPS). The electrical characteristics of the HfOx/TiN RRAM device were analyzed on an Agilent 4156C semiconductor parameter analyzer. Bias voltage was applied on the top electrode with a grounded TiN bottom electrode. All the measurements were performed at room temperature.

Results and Discussion

The typical I-V curves of the two samples in semi-logarithmic and logarithmic form are shown in Figs. 1(a) and 1(b). To simplify the representation, the two samples were abbreviated as PHT for Pt/HfOx/TiN and THT for Ti/HfOx/TiN. Positive voltage was applied to the top electrode of the capacitor, while the TiN bottom electrode was grounded. Before the operation, forming process was needed for all samples. The purpose of forming process was to initiate the switching properties of all HfOx/TiN RRAM devices. Solid and empty symbols stood for the Off to On state and On to Off state switch respectively. In Figs. 1(a) and 1(b), it is clearly observed that the compliance current for THT was larger than that of the PHT sample. THT had to be set at 3 mA to attain a stable switching while PHT only needed 35 μA to attain a stable switching. It is quite interesting that when only 100 μA compliance current was set for the THT sample, no resistive switching behavior could be observed from the sample, and the conducting current reached the 100 μA compliance current. In Fig 1(b), the logarithmic plots of the I-V curves reveal the distinction between the conducting currents of the two samples. The linear correlation between log I and log V, with a slope of 1 indicating the conduction mechanism, was dominated by ohmic conduction. The conducting current of PHT could only be fitted to the ohmic conduction on low resistance state (LRS), and the THT sample could only be fitted at low voltage bias on both HRS and LRS.

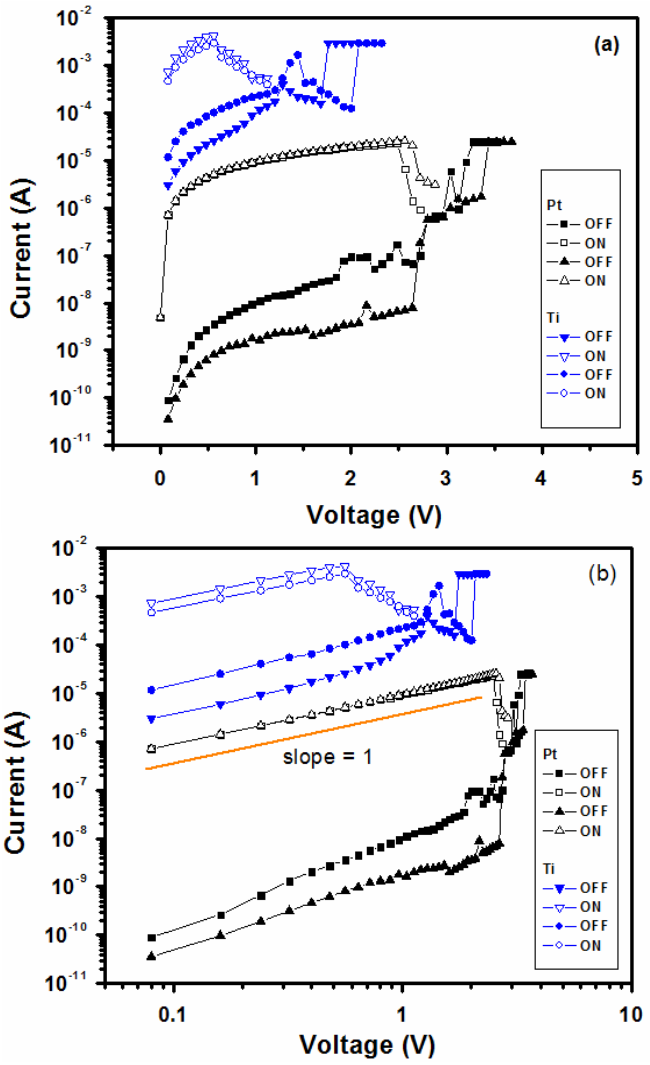

Figure 1. Resistive switching characteristics of the I-V curve of the metal/HfOx/TiN capacitor (a) log I-linear V scale, (b) log I-log V scale. Solid and empty symbols stand for the Off to On state and On to Off state respectively.

A low power operation is a representative advantage of RRAM devices. However, the THT sample did not exhibit low power consumption. Kim et al. (10) proposed that rupture of the filamentary paths occur at about 3-10 nm beneath the anode electrode. They claimed that the HRS current is affected by the thickness or quality of the rupture portion of the TMO film. In our experiments, two samples showing different electrical behaviors seem to imply that the effect of the top electrode to the HfOx film also differs. Lee et al. (8) demonstrated that the carrier injection behavior at HRS in Ru/HfOx/TiN RRAM devices is characterized by a Fowler-Nordheim (FN) tunneling at high bias. It suggests that there exists a thin potential barrier blocking the current transport. As the device was switched back to the HRS, a thin potential barrier layer near the anode was recovered by the partial rupture of filaments near the anode/HfOx interface. The J/V^2 vs. 1/V curve is presented in Fig. 2. The linear line with a negative slope at the large bias

shows that the HRS current at the large bias was due to the Fowler-Nordheim (F-N) tunneling in the PHT sample. This behavior was not observed in THT samples. The distinction of the conduction behavior between PHT and THT shows evidence of the different interfacial layers. It seems that the thin potential barrier in the interface was affected or destroyed to induce large leakage current in HRS. Therefore, THT could not operate at the μA compliance current range.

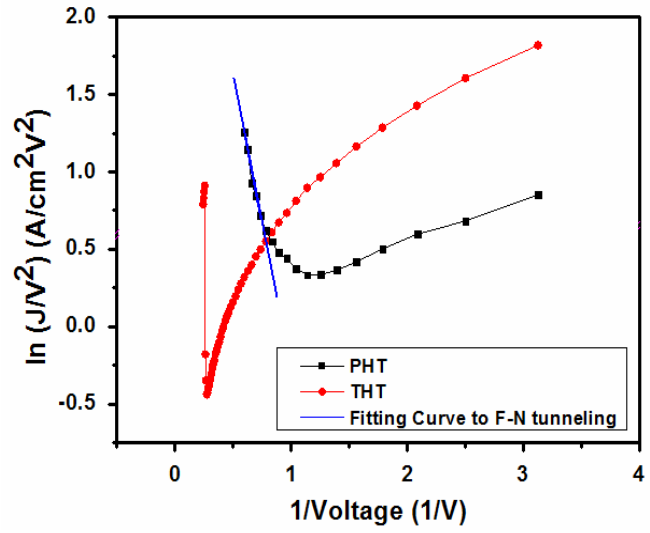

Figure 2. Study of the conduction mechanism in the J/V^2 – 1/V plot. A straight line with negative slope indicates the Fowler-Nordheim tunneling transport.

The reason for the distinction of the HfOx film might be the difference in the free energy of oxidization. Ti is a reactive metal, and it could easily interact with oxygen ions during consecutive switching. Evidence of the interaction between Ti and HfOx interface was found by a series of XPS depth profile analysis shown in Figs. 3(a) and 3(b). Among the depth profiles, 4 spectra lines (A,B,C, and D) near the interface were chosen for observation of the composition of the thin film. For the THT sample, the peak of the Ti spectra were located at 454.1 and 460.1 eV, representing the metal Ti $2p_{3/2\text{-}1/2}(Ti^0)$. A wide distribution of the Ti 2p spectra from Ti^0 towards the side of higher binding energy, stood for the oxidation of the Ti metal in the interface [spectra C in Fig. 3(a)]. Although the XPS could not exactly point out the thickness of the interfacial thin film due to the instrument limitation, the bonding shift only found in the interface compared with the metal Ti spectra undoubtedly already indicated the interaction. For the Pt sample, peak of the metal Pt $4f_{7/2\text{-}5/2}$ lay at 71.1 and 74.6 eV, and there was no peak shift in this sample. It is understandable that metal Pt did not easily oxidize with oxygen ions. The distinction between the XPS depth profile spectra of Pt and Ti are clearly observed in Figs. 3(a) and 3(b), and it might be the reason for the difference in the switching properties between the two metal top electrodes.

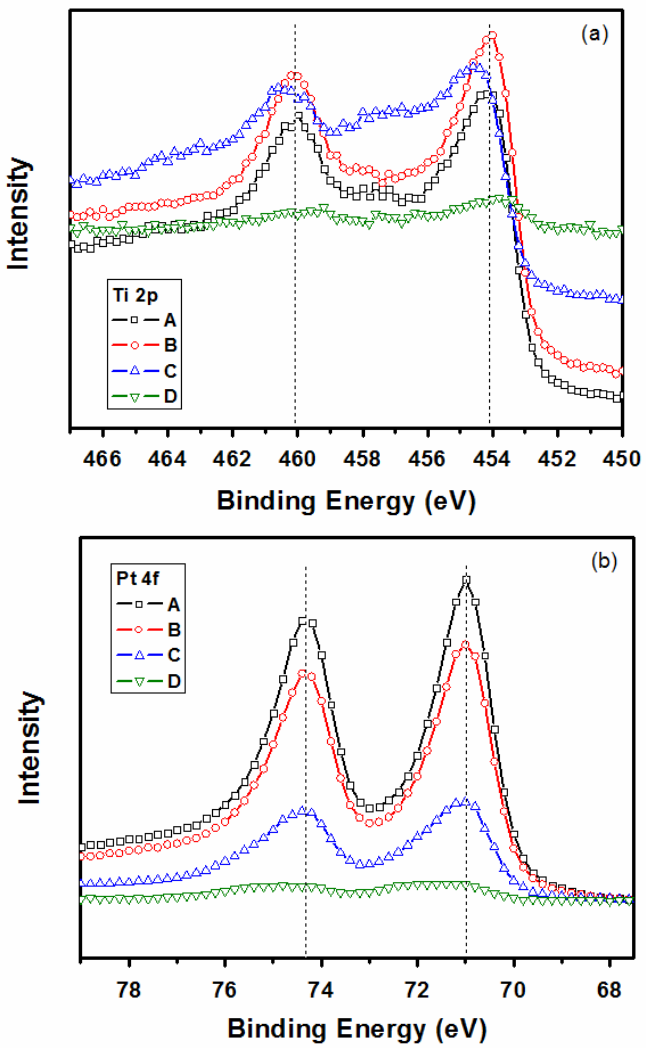

Figure 3. A series of depth profile (A-D) obtained by X-ray photoelectron doublet spectra of (a) Ti $2p_{3/2}$ and Ti $2p_{1/2}$, and (b) Pt $4f_{7/2}$ and Pt $4f_{5/2}$. Curve A, B, C, and D represent the positions from the top electrode to the HfOx film.

For HfOx RRAM devices, the filament model is the fundamental mechanism for explaining the switching behavior. When applying positive bias, oxygen ions are extracted to the M/O interface, forming conducting filaments for the RRAM device from HRS to LRS. Consecutively applying positive bias in LRS allows large current to mediate through the filaments and lead to joule heating. A high temperature inside the conducting filament results in the redistribution of the oxygen ions and the rupture of the filament. This is the well-known filament model. With the use of Pt, oxygen ions extracted from HfOx during the positive operation could easily go back to the vacant site to re-oxidize with the Hf metal during RESET operation. Oxygen ions are free within the metal Pt due to no (or less) reaction or bonding during switching. This demonstrates the advantages of operating at low compliance currents and attaining low power consumption. With the THT sample, however, the behavior was quite different. The reactive metal influenced the oxygen ions in the underlying HfOx film, leading to a variation of the

quality of the film (Fig. 2). It led to larger leakage current in the THT sample and forced the required compliance current to be set higher. Although the conduction mechanism was quite different in HRS, it was almost the same as the LRS. All the samples showed both ohmic conduction with a slope of 1 [Fig. 1(b)]. Induction of metallic filaments in HfOx by a set process for all the samples might be a possible conducting behavior. Since the filaments formed, electrons could mediate through the metallic Hf^{4+} or oxygen defects to enable conduction.

The Pt sample showed a large resistance ratio of about 2 orders of magnitude (Fig. 4). A large Off resistance fluctuation might be attributed to the random redistribution of oxygen ions during the rupture of the conducting filaments by joule heating. A lower resistance, coming from a larger operation current, was observed on both HRS and LRS in the THT sample. A variation of the operation voltage with different top electrodes is shown in Figure 5. The fluctuation in RRAM device is a critical issue which might lead to read-out disturbance or reliability problems. Here, we discuss the fluctuation of the operation voltage. In Figure 5, the box and line shape in each condition represents the case in 25-75% and 5-95% of the data. A larger fluctuation in the set voltage was observed in all samples. The Pt device showed a serious overlap of the operation voltage of SET and RESET, but in the THT sample, a smaller fluctuation and larger operation window were observed. The RESET voltage in the THT sample even showed only 0.5 V dispersion. Jung et al. (11) reported that a Ni-Pt phase formed in the Pt/NiO interface resulting in some defects in NiOx film, which facilitates the switching behaviors. A strong electric field dropped on a weak point, which contributed to the formation and rupture of filaments at a fixed point. Here, we suggest that Ti-O bonding in the interface possibly played a role similar to Ni-Pt. The interfacial layer TiOy/HfOz with a poor quality demonstrated the effect of contributing more defects for facilitation of electron conduction. Therefore, dispersion of the operation voltage could be greatly alleviated. This result also agrees well with the reports by Lee et al. (8) The oxygen contents at the M/O interface were decreased, corresponding to a lower potential barrier and resulting in a lower operation voltage. The top electrode for RRAM device, needs to be investigated in detail for further practical usage.

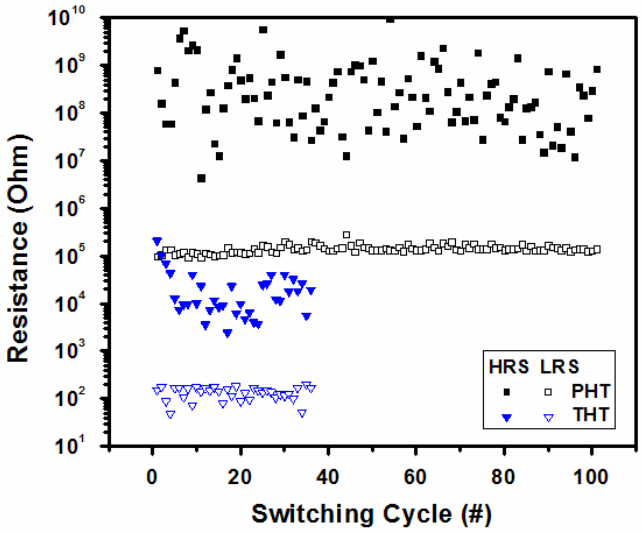

Figure 4. Resistance of the two samples in HRS and LRS state at V=0.4V.

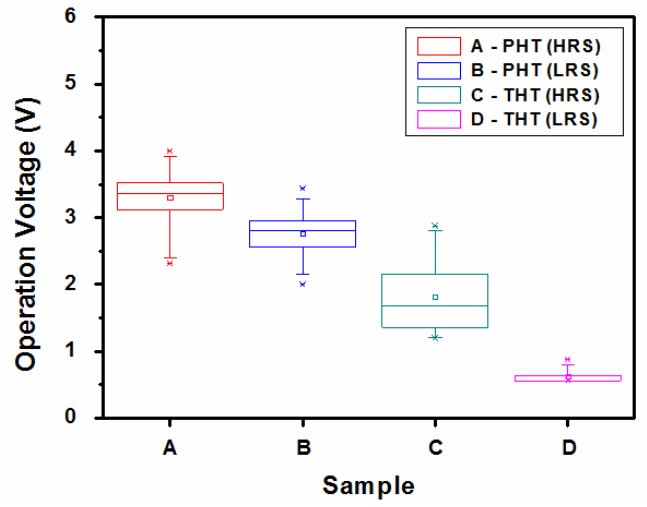

Figure 5. Voltage distribution of the two samples in HRS and LRS state at V=0.4V.

Conclusion

HfOx/TiN RRAM devices with Pt and Ti as the top electrodes are successfully fabricated, and different switching characteristics are observed. Pt/HfOx demonstrates the advantages of low power operation. However, a larger operation current is observed in the Ti/HfOx sample. From the electrical fitting curve, the current injection behaviors are observed to be different for the two samples. A thin potential barrier is observed in the Pt/HfOx interface, which exhibits Fowler-Nordheim tunneling at high bias. This was not observed in the Ti/HfOx sample. Reactive metal Ti interacts with the underlying HfOx surface, resulting in the destruction of the thin potential barrier and the loss of its function for clamping high current. The electrode influences not only the operation current but also the resistance ratio and voltage fluctuation. The trade-off between low voltage fluctuation and low operation current is a critical issue, and it needs further investigation in order to determine the adequate electrode for HfOx RRAM device.

Acknowledgments

This work was supported by J. P. Lin in Nanya Technology Corporation and by M. J. Tsai, P. S. Chen and H. Y. Lee in the Electronics and Optoelectronics Research Laboratory of Industrial Technology Research Institute and by the National Sciences Council (NSC 97_2221_E_182005).

References

1. I. G. Baek, M. S. Lee, S. Seo, M. J. Lee, D. H. Seo, D. –S. Suh, J. C. Park, S. O. Park, H. S. Kim, I. K. Yoo, U. -I. Chung, and J. T. Moon, *IEDM, Tech. Dig.*, 2004, p. 587.

2. C. Rohde, B. J. Choi, D. S. Jeong, S. Choi, J. S. Zhao, and C. S. Hwang, *Appl. Phys. Lett.*, **86**, 262907 (2005).
3. S. Kim, I. Byun, I. Hwang, J. Kim, J. Choi, B. H. Park, S. Seo, M. J. Lee, D. H. Seo, D. S. Suh, Y. S. Joung, and I. K. Yoo, *Jpn. J. Appl. Phys.*, **44**, L345 (2005).
4. S. Seo, I. S. Byun, M. J. Lee, D. C. Kim, S. E. Ahn, B. -H Park, Y. S. Kim, I. K. Yoo, I. R. Hwang, S. H. Kim, J. -S. Kim, J. S. Choi, J. H. Lee, and S. H. Jeon, *Appl. Phys. Lett.*, **87**, 263507 (2005).
5. C. Y. Lin, C. Y. Wu, C. Y. Wu, T. C. Lee, F. L. Yang, C. Hu, and T. Y. Tseng, *IEEE Electron Device Lett.*, **28**, 366 (2007).
6. C. B. Lee, B. S. Kang, A. Benayad, M. J. Lee, S. -E. Ahn, K. H. Kim, G. Stefanovich, Y. Park, and I. K. Yoo, *Appl. Phys. Lett.*, **93**, 042115 (2008).
7. H. Y. Lee, P. S. Chen, C. C. Wang, S. Maikap, P. J. Tzeng, C. H. Lin, L. S. Lee, M. J. Tsai, *Jpn. J. Appl. Phys.*, **46**, 2175 (2007).
8. H. Y. Lee, P. S. Chen, T. Y. Wu, C. C. Wang, P. J. Tzeng, C. H. Lin, F. Chen, M. J. Tsai, C. Lien, *Appl. Phys. Lett.*, **92**, 142911 (2008).
9. S. Lee, W. G. Kim, S. W. Rhee, and K. Yong, *J. Electrochem. Soc.*, **155**, H92 (2008).
10. K. M. Kim, B. J. Choi, Y. C. Shin, S. Choi, and C. S. Hwang, *Appl. Phys. Lett.*, **91**, 012907 (2007).
11. R. Jung, J.-S. Kim, M. –J. Lee, B. H. Park, S. Seo, D. C. Kim, G. S. Park, K. Kim, S. Ahn, Y. Park, I. –K. Yoo, *Appl. Phys. Lett.*, **91**, 022112 (2007).